International Journal of Nanomedicine

Dovepress
open access to scientific and medical research

Open Access Full Text Article

ORIGINAL RESEARCH

Liposomes Loaded with 5-Fluorouracil Can Improve the Efficacy in Pathological Scars

Yixin Li[1–6,*], Qi Sun[2,3,7,*], Lingjia Hao[1,8], Han Shan[2,3,7], Zixi Jiang[1–6], Ying Wang[1–6], Zeyu Chen[2,3,7], Wu Zhu[1–6], Shuang Zhao[1–6]

[1]Department of Dermatology, Xiangya Hospital, Central South University, Changsha, 410008, People's Republic of China; [2]Furong Laboratory (Precision Medicine), Changsha, 410008, People's Republic of China; [3]National Engineering Research Center of Personalized Diagnostic and Therapeutic Technology, Xiangya Hospital, Central South University, Changsha, 410008, People's Republic of China; [4]Hunan Engineering Research Center of Skin Health and Disease, Xiangya Hospital, Central South University, Changsha, 410008, People's Republic of China; [5]Hunan Key Laboratory of Skin Cancer and Psoriasis, Xiangya Hospital, Central South University, Changsha, 410008, People's Republic of China; [6]National Clinical Research Center of Geriatric Disorders, Xiangya Hospital, Central South University, Changsha, 410008, People's Republic of China; [7]School of Mechanical and Electrical Engineering, Central South University, Changsha, 410083, People's Republic of China; [8]Xiangya School of Medicine, Central South University, Changsha, 410083, People's Republic of China

*These authors contributed equally to this work

Correspondence: Shuang Zhao; Wu Zhu, Department of Dermatology, Xiangya Hospital of Central South University, 87 Xiangya Road, Kaifu District, Changsha, Hunan Province, People's Republic of China, Email shuangxy@csu.edu.cn; zhuwuxy@csu.edu.cn

Introduction: Pathological scars, such as hypertrophic scars and keloids, are characterized by the proliferation of fibroblasts and the deposition of collagen that often cause pruritus, pain, and disfigurement. Due to their high incidence and deformity, pathological scars have resulted in severe physical and psychological trauma for patients. Intralesional injection of 5-fluorouracil (5-Fu) is a recommended option for treating pathological scars. However, the efficacy of 5-Fu injection was limited and unstable due to limited drug penetration and short retention time.

Methods: Liposomes are promising carriers that have advantages, such as high biocompatibility, controlled release property, and enhanced clinical efficacy. Here, we constructed a transdermal 5-Fu-loaded liposome (5-Fu-Lip) to provide a more effective and safer modality to scar treatment.

Results: Compared to 5-Fu, 5-Fu-Lip showed superior ability in inhibiting primary keloid fibroblasts proliferation, migration, and collagen deposition, and also significantly inhibited human umbilical vein endothelial cells (HUVECs) proliferation and microvessel construction. *In vivo* experiments demonstrated that 5-Fu-Lip can significantly reduce the severity of hypertrophic scars in a rabbit ear wounding model.

Discussion: 5-Fu-Lip provides a promising strategy to improve drug efficacy, which has great potential in the treatment of pathological scars.

Keywords: liposome, pathological scar, 5-fluorouracil, fibroblast

Introduction

Pathological scars, such as hypertrophic scars and keloids, are the result of abnormal wound healing processes. At the microscopic level, these scars involve hyperproliferation and dysregulation of signaling pathways, leading to excessive collagen deposition.[1] This process primarily affects keratinocytes, fibroblasts,[2] endothelial cells, immune cells,[2] as well as signaling molecules and the associated extracellular matrix (ECM) components. The global impact of pathological scars is significant, affecting billions of individuals worldwide. Studies have reported that hypertrophic scars occur in approximately 35% of linear surgical wounds and up to 72% of burn wounds.[3] Keloids also affecting 4.5–16% of the human population.[4] The management of scars in the United States (US) costs more than $20 billion per year, which is likely much higher worldwide.[5,6] Patients with scars often suffer from severe side effects, such as aesthetics, redness, pain or itching, seriously affecting quality of life.[7] Therefore, an effective therapeutic modality for pathological scars is necessary.

Received: 5 March 2024
Accepted: 11 July 2024
Published: 19 July 2024

According to existing guidelines, intralesional drug injection is recommended as the first-line therapy for scars.[8] This option is not only less invasive but also more cost-effective and accessible compared to surgical excision and laser ablation.[9,10] Common injectable medications include Corticosteroids, Fluorouracil (5-Fu), and Bleomycin. Although corticosteroids have been effective for most patients, they have also been associated with troublesome side effects, including hormonophobia, hypopigmentation, subcutaneous fat atrophy, telangiectasias, rebound effects and ineffectiveness.[11] Bleomycin is often used as an adjuvant therapy in combination with other treatments because of its potent antitumor effects and severe side effects caused by overdose.[12] Several studies have reported using intralesional Botulinum toxin (BTX) injection to treat keloids or hypertrophic scars.[13] However, the effectiveness of this therapy and the mechanism by which it improves pathological lesions remain unclear. 5-Fu, a common chemotherapeutic agent, is often utilized to inhibit tumor cell growth by locking both DNA and RNA synthesis.[14] It is also recommended as an injection option for treating pathological scars,[8] since it can inhibit the proliferation of fibroblasts and the deposition of collagen.[15] A recent study demonstrated that ~85% of keloid patients exhibited more than a 50% improvement after receiving 12 months of intralesional injections of 5-Fu.[16] However, the efficacy of 5-Fu injection was limited and inconsistent.[17] The presence of endogenous dihydropyrimidine dehydrogenase may rapidly remove 5-Fu in tissue, resulting in a short residence time.[18] Additionally, the density of the pathological tissue might hinder the penetration of 5-Fu, which could lead to varying degrees of side effects even with high-dose infection, including extreme pain, ulcerations, and hyperpigmentation.[19,20]

Biomaterials, especially nanomaterials, have achieved many results in assisting the treatment of diseases.[21,22] Liposomes have been the first nanoformulation to be licensed for clinical use.[23] They are also biocompatible and biodegradable drug delivery systems, which can provide a slow and continuous release of drugs within targeted tissues.[24] Due to their efficient and targeted drug release, the same therapeutic effect can be achieved at a lower dose, reducing the cytotoxicity to normal tissues.[25] For example, Wang et al, prepared a paclitaxel-cholesterol-loaded liposomes, that can inhibit the growth and invasion of keloids with minor toxicity.[26] This provides ideas for modifying 5-Fu to improve scar efficacy. In terms of liposome preparation technology, our team also has a certain research base. Shan et al developed a targeted ICG-loaded liposomes using a versatile microfluidic mixing device, showing enhanced photoacoustic imaging and photothermal therapy capabilities.[27]

In this study, we aim to investigate the therapeutic efficacy of liposomes loaded with 5-Fu in pathological scars and suggest its potential for clinical application, hoping to provide ideas for optimizing the treatment of pathological scars and reducing side effects in patients.

Materials and Methods

Chemicals

The drugs used in the assays were 5-fluorouracil (5-Fu, MedChemExpress, HY-90006). 1.2-Dipalmitoyl-sn-glycero -3-phosphocholine (DPPC), 1.2-distearoyl-sn-glycero-3- phosphoethanolamine-N-[amino(polyethylene glycol)2000] (DSPE-PEG2000), and cholesterol were purchased from AVT (Shanghai) Pharmaceutical Technology Co., Ltd., China. Ethanol was purchased from Hunan Huihong Reagent Co., Ltd., China. GR resin was obtained from BMF Precision Technology Inc., China. Dialysis bags were obtained from Hunan Yibo Biological Co., Ltd., China.

Synthesis and Characterization of 5-Fu-Lip

DPPC, DSPE-PEG2000, and cholesterol were dissolved in ethanol at a molar ratio of 70/5/25. 5-Fluorouracil was dissolved in ultrapure water at a concentration of 3 mg/mL. The lipid solution and the 5-fluorouracil solution were introduced into the lipid phase and aqueous phase inlets of the microfluidic chip using a dual-channel micro-injection pump. The ratio of lipid phase to aqueous phase was 1:4, and the total flow rate was 30mL/h. The lipid phase was squeezed and diffused by the two-sided aqueous phase to form a narrow-mixed solvent zone. When the alcohol content of the mixed solvent zone was lower than the alcohol content required for lipid dissolution, the lipid molecules would self-assemble to form a bilayer phospholipid membrane and further form spherical liposomes, which encapsulated the 5-fluorouracil molecules in the aqueous phase. The collected liposome solution was placed in a dialysis bag and dialyzed in pure water to remove ethanol and unencapsulated 5-fluorouracil (Figure 1a). 5-Fu-Lip morphology was observed under a transmission electron microscope (TEM) (Talos™ F200X, Thermo Fisher Scientific, Waltham, MA, USA). The dynamic light scattering and electrophoretic light scattering are the most common methods

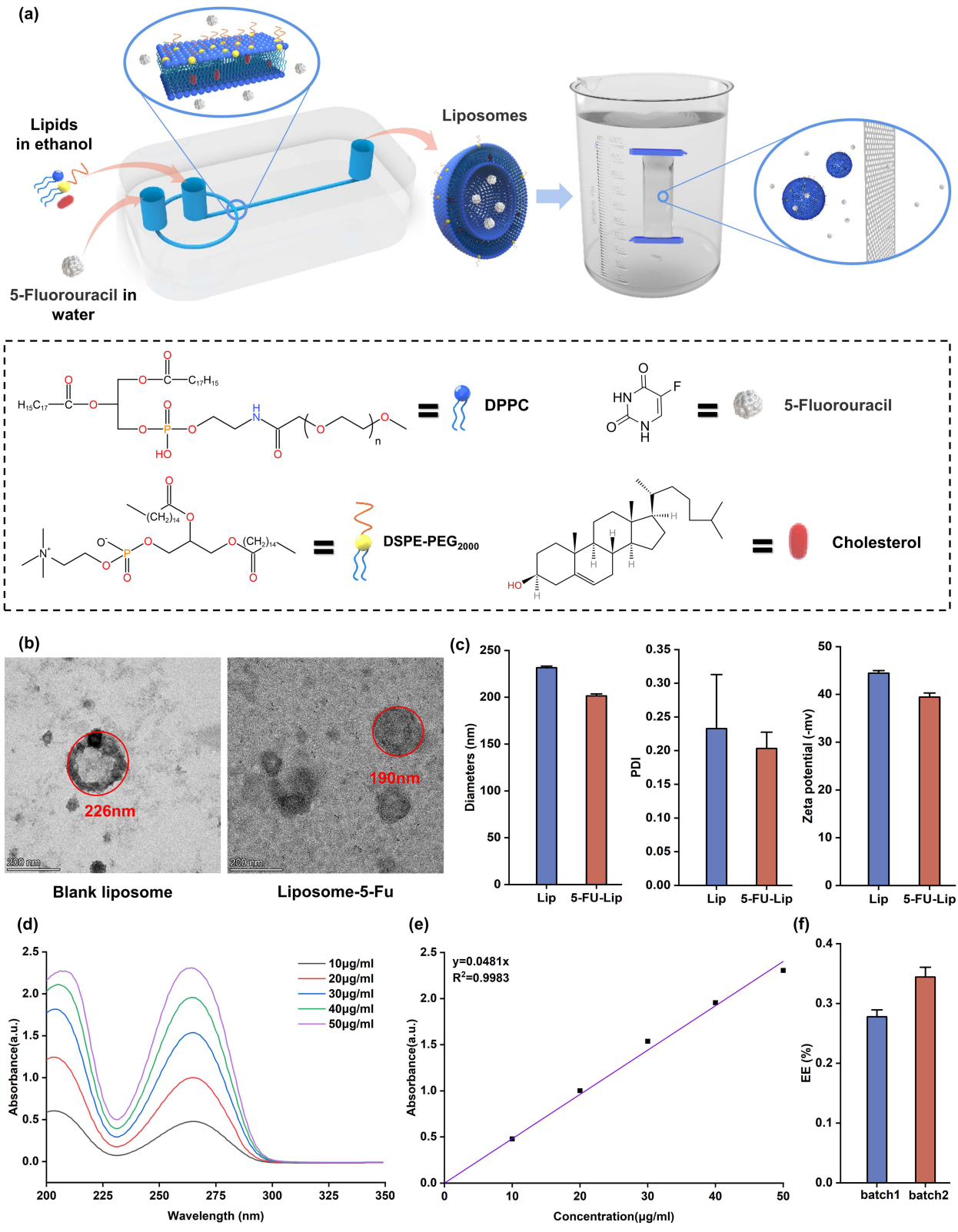

Figure 1 Preparation and characterization of 5-Fu-Lip. (**a**) A schematic diagram illustrating the synthesis of 5-Fu-Lip. (**b**) TEM analysis of the morphology of the blank liposomes and 5-Fu-Lips. (**c**) Characteristics of blank liposomes and 5-Fu-Lips. (**d**) UV-vis spectra of MB solution with a series of concentrations. (**e**) Calibration curve obtained by measuring the absorbance values at 265 nm. (**f**) Encapsulation efficiency of 5-Fu-Lip in two batches. Data are presented as the mean ± SD. (n=3).

for detecting the average size, polydispersity index (PDI) and zeta potential of nanoparticles. 5-Fu-Lip solution was diluted with distilled water 10 times and the average size, PDI and zeta potential were detected with a BeNano 90 + BeNano Zeta (Dandong Bettersize Instruments Ltd, Dandong, China).

Cell Lines and Cell Culture

Human foreskin fibroblasts (HFF-1) and Human umbilical vein endothelial cells (HUVECs) were obtained from Hunan Engineering Research Center of Skin Health and Disease (Changsha, China). HFF-1, HUVECs, and PKFs (Primary keloid fibroblasts) were cultured in Dulbecco's Modified Eagle Medium (DMEM, BasalMedia, L110KJ) supplemented with 10% Fetal Bovine Serum (FBS, ExCell, FCS500) and 1% penicillin streptomycin solution (BI, 03–031-1B), which was also referred to as complete medium later, in a humidified incubator at 37°C with 5% CO_2. Cells were subcultured via trypsinization once reaching a confluency of ~90% . Passages of 2 to 6 cells were used for experiment.

Isolation of Primary Keloid Fibroblasts (PKFs)

With ethical approval (No.202305092, the Medical Ethics Committee of Xiangya Hospital), human keloid tissues were obtained from the Department of Dermatology, Xiangya Hospital, Central South University. Patients included in this study have provided informed consents, in accordance with the Declaration of Helsinki. The protocol of PKFs extraction referred to He Y et al[28] with several modifications (Figure S1). The human keloid tissues were soaked in DMEM (BasalMedia, L110KJ) and transported to the laboratory in ice. The epidermis and fat layer of keloid tissues were removed with only dense dermis remained. The remained dermis was cut into 3mm*3mm*3mm pieces and placed evenly in T25 cell culture flasks (ExCell, CS016-0104), with about 1 cm spacing between pieces. 1 mL complete medium was added to the culture flask. Then, tissues were incubated in a humidified incubator at 37°C with 5% CO_2. After 24 hours, 2 to 3 mL of complete medium were added to the culture flask. Thereafter, the medium was changed every 3 days. Most of PKFs would crawl out of the tissues after 15 days of culture.

Cell Proliferation Assay

HFF-1, PKFs and HUVECs were incubated in complete medium in a humidified incubator at 37°C with 5% CO_2. 1.0×10^4 cells (As for HUVECs, 8.0×10^3 cells would be better) were seeded into individual wells of 96-well plates and cultured for 24 h. The free 5-Fu and 5-Fu-Lip were diluted with medium containing serum and divided into five groups (10.0, 20.0, 50.0, 100.0, 200.0 μg/mL). Next, 100μL of the sample solutions were added to the cell medium, while cells treated with pure medium were used as the control. After incubation for 24 hours and 36 hours, cell viability was measured at 450 nm using a Cell Counting Kit-8 (CCK-8, Selleck, B34302) cell proliferation and toxicity detection kit. The half maximal inhibitory concentration (IC50) was counted by GraphPad Prism software.

Scratch Wound Healing Assay

PKFs cells were cultured in 6-well plates with a density of 4.0×10^5 cells per well. After reaching 80–90% confluency, a straight line was scratched on the cell monolayer with a 10μL pipette tip. Then, cells were washed with Dulbecco's phosphate-buffered saline (DPBS, BI, 02–023-1A) to remove debris and then replenished with 2.0 mL serum-free medium or appropriate drug solutions. Drug solutions including free 5-Fu (100.0 μg/mL) and 5-Fu-Lip (100.0 μg/mL) in pure DMEM. Cell migration was recorded with a microscope and the scratched area was analyzed with ImageJ.

Transwell Migration Assay

For the vertical migration assay, a Transwell experiment was performed with 8 μm pore chambers inserted into 24-well plates (Corning, NY, USA). PKFs were obtained, resuspended in serum-free medium, medium containing free 5-Fu (100.0 μg/mL) and 5-Fu-Lip (100.0 μg/mL), respectively, at a concentration of 5×10^4/100 μL and seeded in the upper chambers, while 500 μL of DMEM containing 30% FBS was placed into the bottom chamber as a chemotactic factor. After 24 h, cells were fixed in 4% paraformaldehyde (Servicebio, G1101-500ML) for 15 min at room temperature. Non-motile or non-migrated cells on the top surface of the filter were removed, while motile or migrated cells on the bottom surface were stained with crystal violet.

Endothelial Cell Tube Formation Assay

60 μL Matrigel (Corning, 354234) was precoated into each well of a 24-well plate and polymerized at 37°C for 60 min. Next, HUVECs were resuspended with complete medium, 5-Fu (100.0 μg/mL) and 5-Fu-Lip (100.0 μg/mL), respectively, and seeded with a density of 3.0×10^4 cells/100μL per well. After 6 h of incubation, capillary-like tubes were photographed by a microscope. The total length and nodes number of tubular structures were quantified with ImageJ.

Immunofluorescence Staining and Imaging

PKFs were seeded into 24-well plates at $4–5\times10^4$ cells per well and cultured with complete medium, 5-Fu (100.0 μg/mL) and 5-Fu-Lip (100.0 μg/mL) for 24 h. After that, the cells were rinsed with DPBS twice and fixed with 4% paraformaldehyde for 15 min at room temperature. Then, the cells were permeabilized by 0.5% Triton X-100 (Sangon Biotech, A600198-0500) for 20 min and were blocked by 5% bovine serum albumin (BSA, Genview, FA016) in PBS for 2 h at room temperature. Subsequently, the cells were incubated with a primary antibody against Alpha Smooth Muscle Actin (α-SMA, 1:1000, protein tech, 14395-1-AP), Collagen Type I (Col I, 1:250, protein tech, 14695-1-AP) and Collagen Type III (Col III, 1:250, protein tech, 22734-1-AP) at 4°C overnight. After washing with PBS, the cells were protected from light and incubated with a secondary antibody (Alexa Fluor 594 donkey Anti-rabbit for red, Alexa Fluor 488 donkey Anti-rabbit for green) (1:1000, Invitrogen, A21207 and A21206) for 1 h at room temperature. The cells were washed with PBS again and then incubated with fluoro shield mounting medium with DAPI (Abcam, ab104139) for 10 min at room temperature. Following staining, the cells were imaged using a fluorescence microscope (Nikon, ECLIPSE Ts2R). The Integrated Density (IntDen) and the Area of each image can be measured with ImageJ. Mean fluorescence intensity (Mean) = IntDen/Area.

Quantitative Real-Time PCR (qRT-PCR)

Total RNA was extracted from cells by Magzol reagent (Magen, R4801-01) according to the manufacturer's protocol. cDNA was synthesized using a Hifair® III 1st Strand cDNA Synthesis SuperMix for qPCR Kit (Yeasen, 11141ES60). Quantitative PCR was performed using 2X SYBR Green qPCR Master Mix (Bimake, B21703) following the manufacturer's guideline. GAPDH was used as the internal control. All PCR primers used in this study were bought from Sangon Biotech and were listed in Table S1. The qRT-PCR assays and data collection were performed on a 7500 real-time PCR system (Applied Biosystems, USA). The data were analyzed by using the $2^{-\Delta\Delta CT}$ values.

Protein Preparation and Western Blot

Cells were lysed in RIPA buffer according to the manufacturer's protocol, and protein concentrations were determined by BCA assay. The extracted protein was adjusted to a uniform concentration and denatured at 95°C for 5 minutes. Proteins were segregated on 8% SDSPAGE and migrated to PVDF membranes (Millipore). Then, membranes were incubated with 5% Nonfat-Dried Milk-TBST buffered for blocking followed by primary antibodies overnight at 4°C: mouse anti-β-actin (1:20000, proteintech, 66009-1-LG), mouse anti-GAPDH (1:3000, proteintech, 60004-1-LG), rabbit anti-α-SMA (1:1000), rabbit anti-Col I (1:2000), rabbit anti-Col III (1:1000). Three washes were performed for 10 minutes with TBST. The membranes were incubated with secondary antibodies (1:5000, abclonal, AS003 and AS014) for an hour at room temperature and washed as above. Blots were detected by an imaging system (Odyssey-Fc, Li-Cor, SA).

Pharmacodynamics Studies in Rabbits

The rabbit ear hypertrophic scar model has been widely applied in scar research.[29] Two female New Zealand rabbits (2.0–2.5 kg) were obtained from the Hunan Slac Laboratory Animal (Slac, Hunan, China). All the animal experiments were performed in line with the guidelines of "The Service Manual of the Center of Laboratory Animals, Central South University", as well as in accordance with the National Institutes of Health guidelines for the care and use of laboratory animals. And all procedures were approved by the Animal Care and Use Committee of Central South University. A hypertrophic scar models were successfully constructed after 21 days of recovery and epithelialization. Five scars (1 cm*1 cm) were created on the ventral side of each rabbit ear. In order to eliminate the differences between groups as much as possible, three scars with similar size, thickness, and softness on each ear were selected, and divided into three groups

(n=4): Control group, 5-Fu injection group and 5-Fu-Lip injection group. The control group did not receive any treatment, whereas the injection groups received injections for 10 consecutive days. The drug dose for both injection groups was 0.5mg/mL, and the volume was 100 μL. On the next day after the last administration, the scar tissues were collected. Sections were made across the most elevated portion of the scar and performed with Hematoxylin and eosin (H&E) and Masson staining. For histomorphometric analysis, the scar elevation index (SEI) which measures the ratio of total scar connective tissue area to the area of underlying dermis is assessed.[30] SEI = vertical distance from the highest point of the scar to the surface of the ear cartilage/vertical distance from the surface of the skin on the ventral surface of the ear to the surface of the ear cartilage.

H&E and Masson Staining

Tissue samples were fixed in 4% paraformaldehyde. After dewaxing and hydration, H&E and Masson's staining were performed following operating guidelines.

Statistical Analysis

The two-tailed Student's *t*-test was used to determine the statistical differences between two groups. The one-way ANOVA was used to determine the statistical differences between multiple groups. Statistically significance was represented as: *$p<0.05$; **$p<0.01$; ***$p<0.001$; ****$p<0.0001$. All analyses and data visualization were carried out using GraphPad Prism software (version 9.4.0) as appropriate.

Results and Discussion

Preparation and Characterization of 5-Fu-Lip

5-Fu is a commonly used intralesional injection for treating pathological scars, as it inhibits fibroblast proliferation and collagen deposition.[15,31] However, as a chemotherapeutic drug, it has a short residence time and leads to serious side effects such as ulceration, hyperpigmentation.[19,32] Also, the dense scar tissue limited the penetration depth that affected the clinical application of 5-Fu in scars. Liposome is one of the most commonly used drug delivery systems due to its excellent biocompatibility, satisfactory ability in controlling drug release, and passive targeting capability.[33] In a previous study,[34] triamcinolone acetonide lipid nanoparticles have shown better transdermal permeation properties and milder side effects, which are safe and beneficial for the treatment of hypertrophic scars. A novel elastic liposome containing papain has also been proven to be an excellent topical preparation for hypertrophic scar treatment, resulting in a significant decrease in the scar elevation index, microvascular density, and collagen fiber.[35] Therefore, to enhance the efficacy of 5-Fu and reduce its side effects, we developed liposomes for the delivery of 5-Fu (also known as stealth liposomes, SL). Furthermore, to optimize drug utilization, we employed DSPE-PEG2000 as one of the excipients in liposome preparation (Figure 1a). DSPE-PEG2000 has the capability to form a hydrated membrane on the surface, preventing the adsorption of plasma components and reducing the uptake of liposomes by the reticuloendothelial system. This prolongs the circulation time of liposomes in the body.[36] The drug release results indicate that the release of free 5-Fu is relatively fast, with nearly all the drug released within 60 minutes, reaching a cumulative release percentage of 98.68%. In contrast, 5-Fu-Lip reached its highest cumulative release percentage of 97.02% at 180 minutes (Figure S2). Thus, 5-Fu-Lip exhibits a controlled release effect of 5-Fu and prolongs its residence time.

TEM revealed that the blank liposomes and 5-Fu-Lip exhibited a spherical structure, with average diameters of ≈226 nm and ≈190 nm, respectively (Figure 1b). The particle size, PDI, and zeta potential were also analyzed. The average diameters of the blank liposomes and 5-Fu-Lip were ≈231 nm and ≈201 nm, the PDIs were ≈0.233 and ≈0.203, and the zeta potentials were ≈-44.4 mV and ≈-39.5 mV (Figure 1c). These data indicated that the structure of 5-Fu-Lip is similar to that of blank liposomes, suggesting that excellent biocompatibility and satisfactory drug delivery ability of liposomes are still retained. After one week and two weeks, we tested the particle size, PDI, and zeta potential of 5-Fu-Lip again to demonstrate the stability in vitro. The results showed that there were no significant changes in the characteristics of 5-Fu-Lip (Figure S3), which indicates that the 5-Fu-Lip can maintain stability in solution over a certain period of time. By measuring the absorption spectra of 5-Fu solutions with different concentrations and establishing standard calibration plots (Figure 1d–e), the encapsulation efficiency of 5-Fu-Lip in two batches are 27.29% and 34.43%, respectively.

Microfluidic technology is a novel method for the preparation of 5-Fu-Lip, offering the advantages of precise control and efficient preparation.[37] The microfluidic method makes it easy to regulate the particle size, allowing for the construction of appropriate particle sizes that match different applications. Additionally, the obtained liposome particle size is more uniform and the PDI is smaller.[38] Currently, we have designed a dialysis-type microfluidic chip through 3D printing, which enables the efficient and rapid formation of stable and uniform liposomes (Figure S4).

5-Fu-Lip Inhibits the Growth and Migration of PKFs

Inhibiting the proliferation and migration of scar fibroblasts is an effective strategy for treating scars.[39] To better investigate the inhibitory effects of 5-Fu and 5-Fu-Lip on scars, we extracted PKFs from patient keloid tissue. To confirm that the extracted cells were fibroblasts, we performed immunofluorescence staining of α-SMA and F-action (Figure S5). We assessed cell viability in PKFs and HFF-1, with HFF-1 used as a control to determine the sensitivity of 5-Fu-Lip. When the concentration of 5-Fu ranged from 10μg/mL to 100μg/mL, there were no significant differences in the inhibition of HFF-1 viability caused by both 5-Fu and 5-Fu-Lip. However, when the concentration of 5-Fu exceeded 200μg/mL, 5-Fu-Lip demonstrated a strong inhibitory capability on the proliferation of HFF-1, with cell viability below 50% at 24 h and 36 h *($p<0.05$)* (Figure 2a). Compared to the free 5-Fu group, 5-Fu-Lip significantly decreased cell viability in PKFs at higher concentrations after 24 h and 36 h (Figure 2b). However, 5-Fu-Lip exhibits lower performance than free 5-Fu at lower concentrations (less than 20 ug/mL), which may be related to the stability of 5-Fu and the efficiency of drug release at these concentrations. At low concentrations, the differences between 5-Fu-Lip and free 5-Fu were not statistically significant. After incubating with 5-Fu-Lip at the concentration of 100μg/mL, the inhibition rate reached close to 50%. After 36 h of treatment, PKF viability in both groups decreased to less than 70% at all concentrations. The IC50 was calculated from the cell viability measurements. At 24 h, the IC50 of 5-Fu-Lip for PKFs was lower than that of HFF-1, indicating that scar fibroblasts are more sensitive to 5-Fu than normal fibroblasts (Figure 2c). Meanwhile, the IC50s of 5-Fu-Lip were lower than those of 5-Fu for the same cell lines, suggesting that 5-Fu-Lip can achieve comparable effects to free 5-Fu at a lower concentration. Generally, liposomes have higher cellular uptake efficiency, allowing for better exertion of pharmacological effects and even reduce the toxicity.[40]

Scars usually protrude above the skin surface due to overgrowth and migration of fibroblasts.[41] To assess the inhibition of cell migration, we conducted a wound scratch assay and a transwell experiment to observe the lateral and vertical migration of

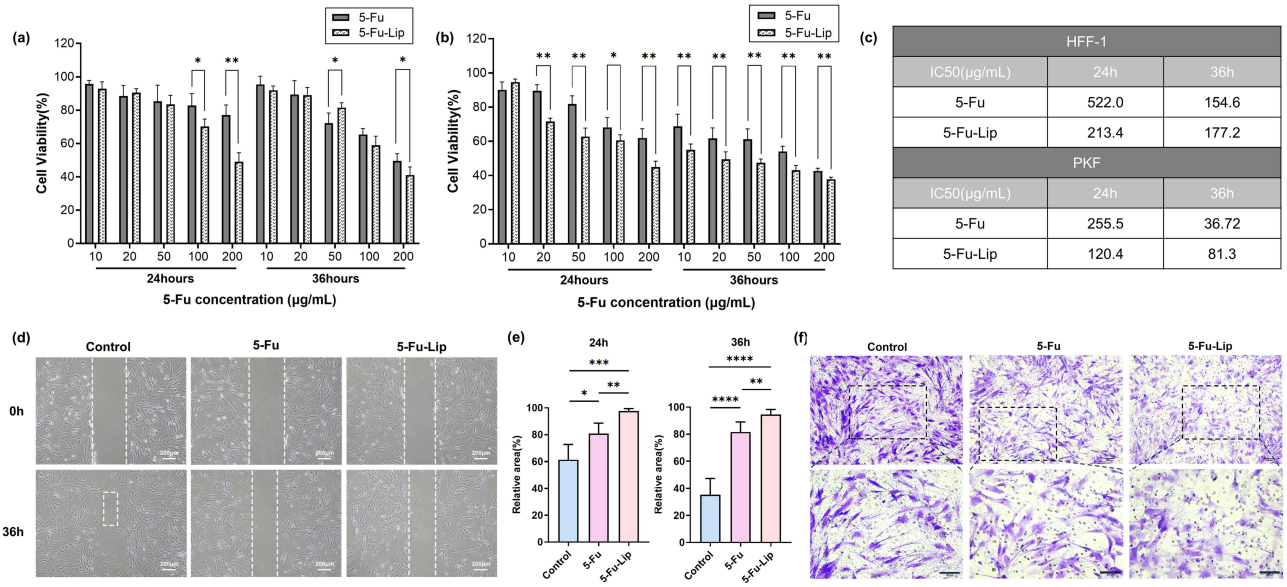

HFF-1		
IC50(μg/mL)	24h	36h
5-Fu	522.0	154.6
5-Fu-Lip	213.4	177.2
PKF		
IC50(μg/mL)	24h	36h
5-Fu	255.5	36.72
5-Fu-Lip	120.4	81.3

Figure 2 Inhibitory effect of 5-Fu-Lip in cell proliferation and migration. Viability comparison of HFF-1 (**a**) and PKFs (**b**) after treated by free 5-Fu and 5-Fu-Lip for 24 hours and 36 hours (n=5). (**c**) IC50 of HFF-1 and PKFs calculated based on previous treatment. (**d**) Representative images of lateral migration in PKFs within 36 hours. Scale bars = 200μm. (**e**) The relative area of the blank space to the original scratch after 24 and 36 hours (n=5). (**f**) Representative transwell images of vertical migration in PKFs within 24 hours. Scale bars = 200μm. (*$p<0.05$; **$p<0.01$; ***$p<0.001$; ****$p<0.0001$).

PKFs. PKFs in the control group showed strong migration, while the lateral migration of 5-Fu-Lip group was significantly inhibited at both 24- and 36-h time points (Figures 2d and S6). After 36 h, the scratch area in the control group was only (35.28 ±12.10)% of the original area, whereas the relative scratch area in the 5-Fu group was (81.58±7.45)%. The migratory behavior of PKFs in the 5-Fu-Lip group was almost completely inhibited, with a relative scratch area of (94.51±3.82)%, which showed noticeable suppression compared to the control and 5-Fu group *(p<0.01)*. In the transwell assay, a large number of PKFs crossed to the lower chamber in the control group, while significantly fewer cells migrated in the 5-Fu and 5-Fu-Lip groups (Figure 2f). Moreover, the morphology of fibroblasts treated with 5-Fu-Lip was altered after crossing the upper chamber, showing star-shaped flat cells under high magnification (Figure 2f), which did not have a myofibroblast morphology. The change in morphology may also be related to their migratory ability.[42]

5-Fu-Lip Inhibits the Formation of Capillary-Like Tubes

Angiogenesis is crucial for efficient tissue restoration during the wound repair process.[43] However, abnormal levels of new blood vessel formation can exacerbate scar formation, leading to dysfunction and pain.[44] Research suggests that reducing angiogenesis is an effective method for improving long-term healing outcomes.[45] Therefore, inhibiting the proliferation of HUVECs and the formation of capillary-like tubes can be beneficial in scar treatment.[46] In our study, 5-Fu-Lip significantly decreased cell viability in HUVECs when the concentration of 5-Fu reached above 50μg/mL after 24 h and 36 h, compared to the 5-Fu group (Figure 3a). The IC50 of 5-Fu-Lip against HUVECs was lower than that of 5-Fu (Figure 3b), indicating that liposome-loaded 5-Fu had a greater pharmacological effect. Moreover, the results of the tube formation assay showed that the number of nodes and total length of capillary-like tubes formed by HUVECs in the 5-Fu-Lip group were significantly reduced compared to both the 5-Fu and control groups (Figures 3c–d, and S7). Overall, these findings demonstrate the potential of 5-Fu-Lip in the treatment of vascular anomalies at a lower dosage.

5-Fu-Lip Inhibits the Collagen Secretion and Deposition

Scar is characterized by a large number of collagen fibers and ECM deposition.[47] Collagen type I (Col I) and collagen type III (Col III) are the main components of ECM, and both Col I and Col III increase in the process of scar

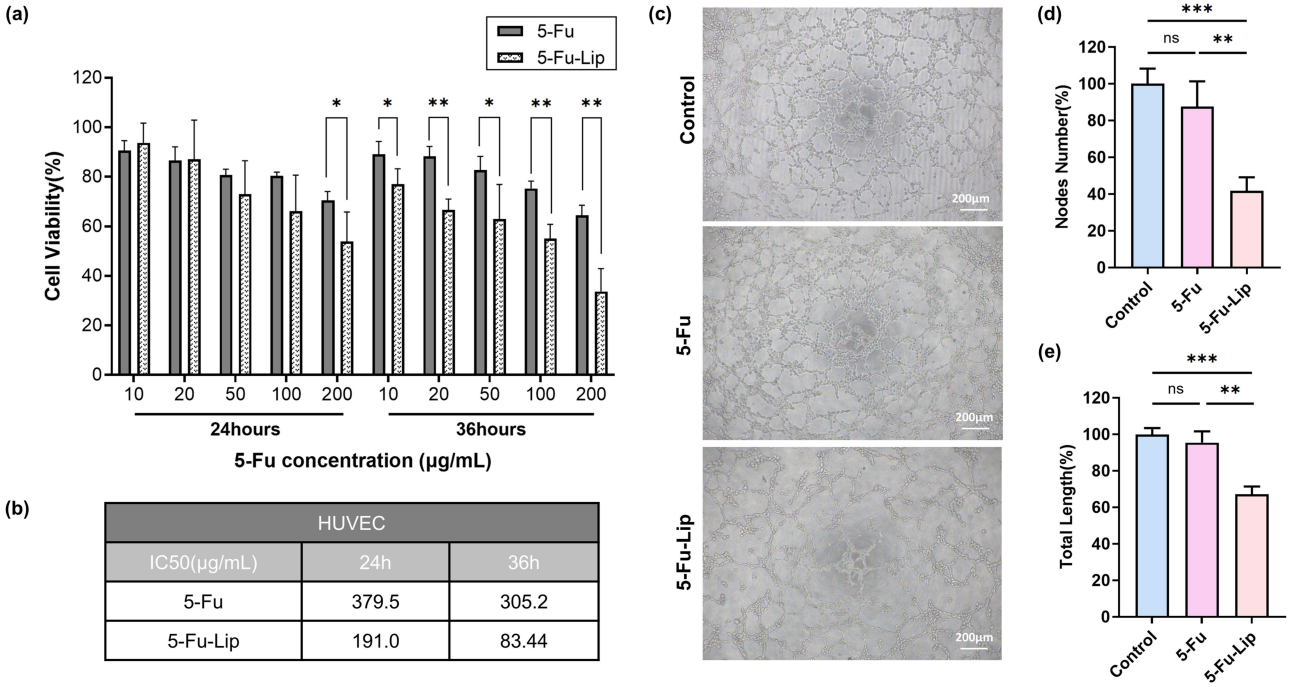

Figure 3 Inhibitory effect of 5-Fu-Lip in capillary-like tube formation. (**a**)Viability of HUVECs after treated by free 5-Fu and 5-Fu-Lip for 24 hours and 36 hours (n=5). (**b**) IC50 of HUVECs calculated based on previous treatment. (**c**) Representative images of tube formations in different groups. Scale bars = 200μm. (**d** and **e**) The percentage of nodes number and total length for HUVECs (n=3). (*p<0.05; **p<0.01; ***p<0.001).

formation.[48,49] α-SMA plays a key role in myofibroblast contraction, scar contracture, and excessive wound healing.[50] Its expression represents the degree of cellular specialization of fibroblasts to myofibroblasts. Thus, we chose Col I, Col III, and α-SMA as indicators of PKFs. The results of qPCR showed that the expression of Col I, Col III, and α-SMA was significantly reduced by 5-Fu-Lip ($p<0.0001$) (Figure 4a). At the protein expression level, Col I, Col III, and α-SMA were also decreased after 5-Fu-Lip treatment (Figure 4d). However, the inhibitory effect of 5-Fu-Lip on α-SMA protein expression was more pronounced than that of 5-Fu, whereas it was not as strong on Col I and Col III protein expression. Immunofluorescence assay showed that Col I and Col III expressed in the extracellular matrix, whereas α-SMA expressed intracellularly (Figure 4c). After 24 h of drug treatment, the number of PKFs and the fluorescence intensity of target proteins were reduced. Quantification of the mean fluorescence intensity revealed that 5-Fu-Lip significantly inhibited the expression of Col I, Col III, and α-SMA (Figure 4b). Compared with 5-Fu, the inhibitory effect of 5-Fu-Lip on α-SMA was more significant, which is consistent with Western blot results.

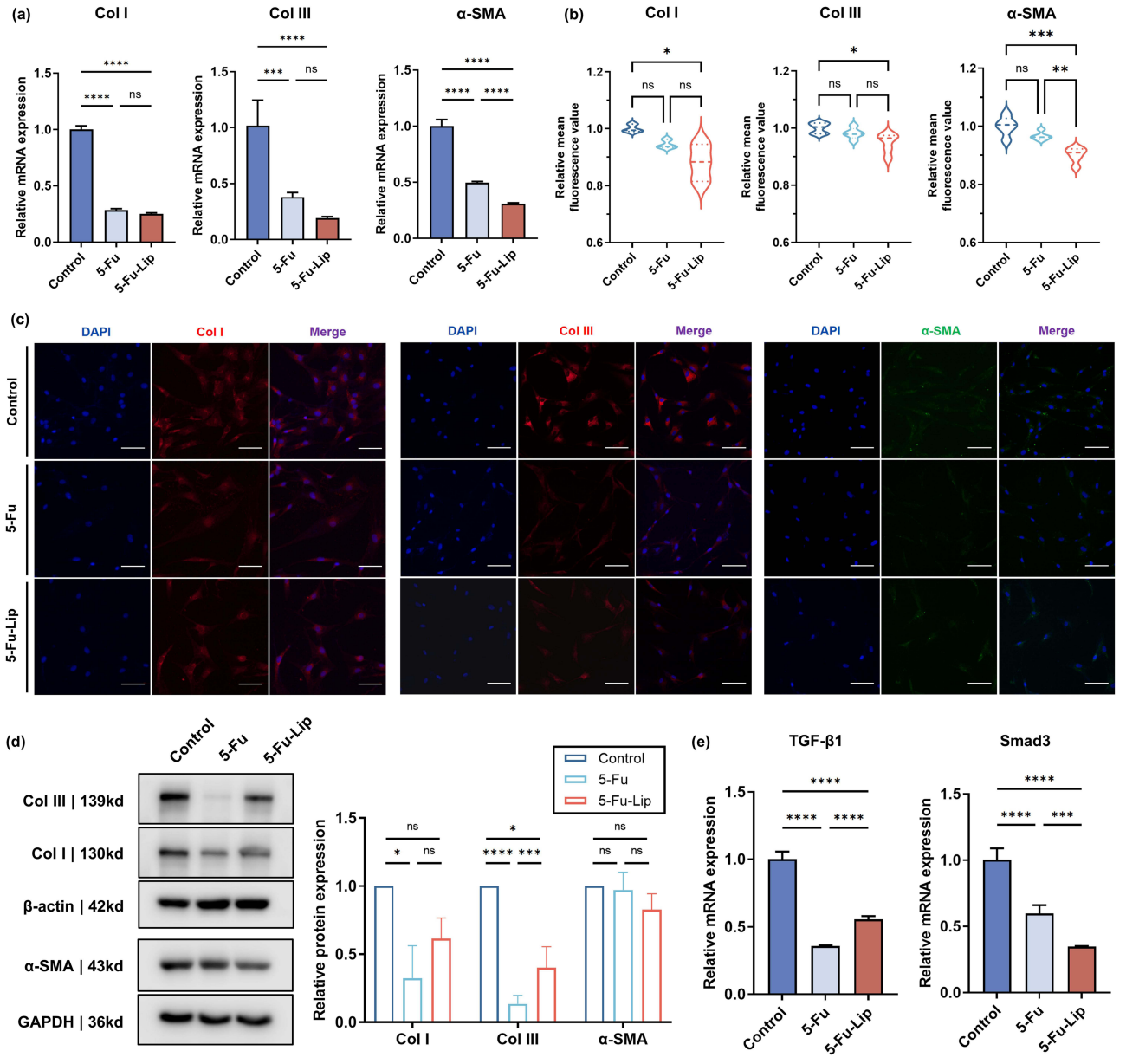

Figure 4 Inhibitory effect of 5-Fu-Lip in collagen secretion. (**a**)The expression of Col I, Col III and α-SMA at mRNA level in different groups (n=4). (**b** and **c**) Fluorescence distribution and density of Col I, Col III and α-SMA in different groups; Scale bars = 200μm. (n=5). (**d**) The expression of Col I, Col III and α-SMA at protein level in different groups (n=3). (**e**) The expression of TGF-β1/Smad signaling at mRNA level (n=4). (*$p<0.05$; **$p<0.01$; ***$p<0.001$; ****$p<0.0001$).

TGF-β1 is involved in various processes including inflammation, angiogenesis, fibroblast proliferation, collagen synthesis, and ECM remodeling. Studies have indicated a close relationship between TGF-β1 and wound healing as well as scar formation.[51] High expression of TGF-β1 has been observed in hypertrophic scar tissue in comparison to scarless tissue.[52] This process is typically regulated by the TGF-β1/Smad signaling pathway.[53] Smad3 has been identified as a significant downstream signaling molecule of TGF-β1 in fibrosis mediation.[54] Additionally, Smad3 can interact with other signaling pathways, such as the ERK/p38[55] and MAPK[56] pathways, to mediate fibrosis. Consequently, its high expression is strongly associated with scar formation. The results of qPCR analysis demonstrated a significant reduction in the expression of TGF-β1 and Smad3 upon treatment with 5-Fu-Lip ($p<0.0001$) (Figure 4a). This suggests that the mechanism of action of 5-Fu-Lip may be related to the TGF-β1/Smad signaling pathway.

In vivo Therapeutic Efficacy of 5-Fu-Lip on Scars

Three weeks after the operation, the wounds had already re-epithelialized and formed scar tissues, which were obviously red and swollen. After 10 days of administration, the scar tissue in the 5-Fu-Lip group appeared flatter compared to both the 5-Fu and control groups. The scar bulges were smoother and the color of the scar tissue was similar to that of surrounding skin (Figure 5b). To analyze the distribution of fibroblast and collagen deposition, H&E and Masson staining were performed. It was observed that the control group and 5-Fu group had a large number of dense fibroblasts and irregularly arranged collagen fibers, while the 5-Fu-

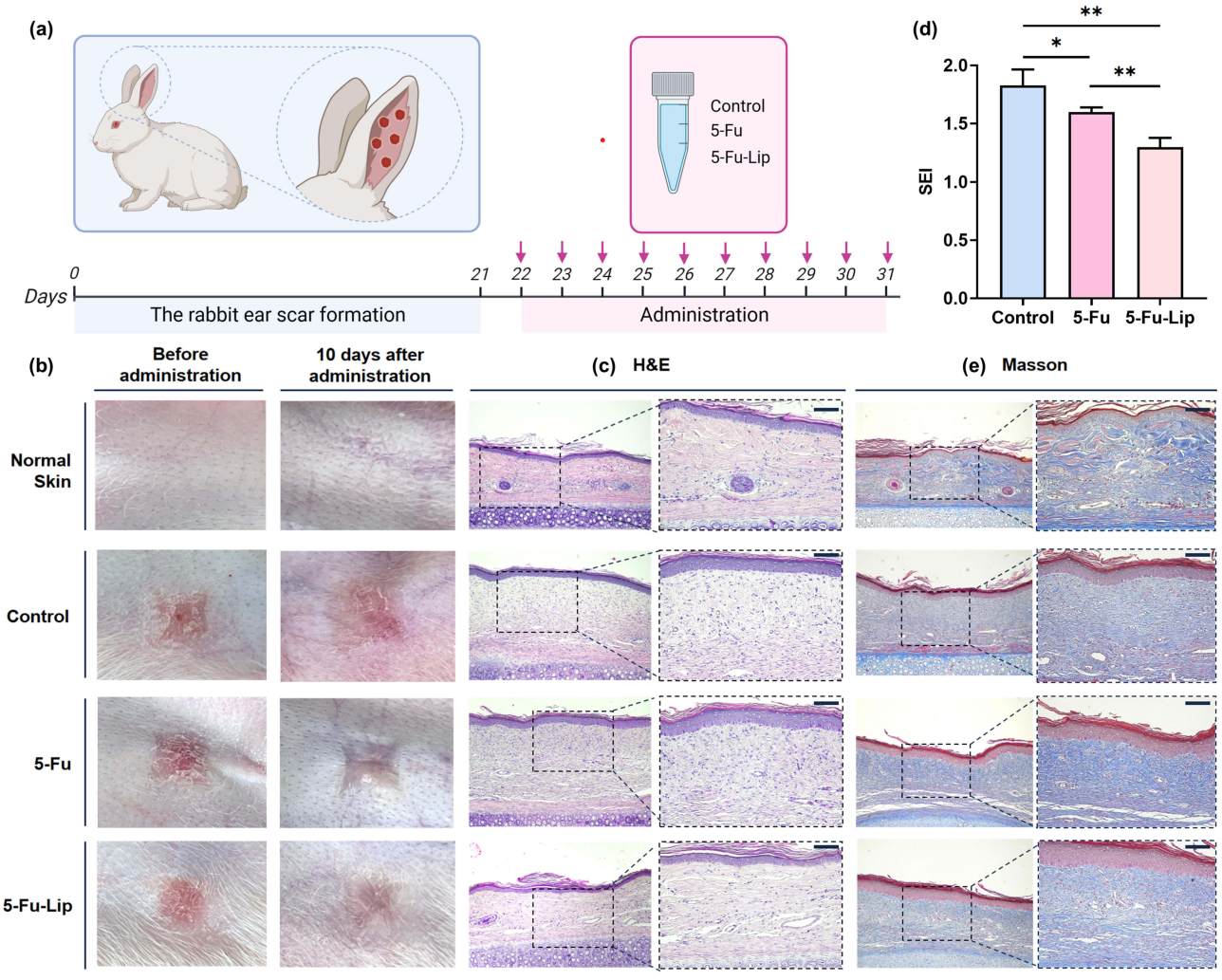

Figure 5 The therapeutic effect of 5-Fu-Lip in rabbit hypertrophic scars. (**a**) A flow chart of the drug injection procedure. (**b**) Representative images of rabbit ear scars before and 10 days after the administration. (**c**) H&E images of rabbit ear scars under different administrations; Scale bars = 200μm. (**d**) Quantification f SEI, (n=5). (**e**) Masson images of rabbit ear scars under different administrations; Scale bars = 200μm. (*$p<0.05$; **$p<0.01$).

Lip group had relatively neat and loose arrangement of fibers (Figure 5c and e). Additionally, the scar thickness was lower in the 5-Fu-lip group, and under low magnification, gland-like structures were observed, resembling normal skin (Figure 5c).[57] To assess the severity of the scar, SEI was used, which is calculated based on H&E images. Importantly, the SEI value was significantly lower in the 5-Fu-Lip group compared to the 5-Fu and control groups ($p<0.01$) (Figure 5d). These results suggest that 5-Fu-Lip can treat scars by suppressing collagen fiber deposition and improving fibroblast alignment. We hypothesize that the mechanism of action of 5-Fu-Lip in the treatment of pathological scars may be related to the properties of liposomes themselves. The surface of the liposome is modified with polyethylene glycol (PEG), which grants the liposome a longer circulation time in the body, lower immunogenicity, and better stability.[36] These modifications help reduce recognition and phagocytosis by the mononuclear phagocyte system (MPS). Thus, 5-Fu-Lip exhibits a controlled release effect of 5-Fu and prolongs its residence time at the lesion compared to free 5-Fu, thereby enhancing treatment efficacy. In addition, liposomes can be taken up by cells through endocytosis.[58,59] With subcutaneous injection of 5-Fu-Lip, the drug bypasses the skin stratum corneum barrier and enters directly into the subcutaneous tissue. This localized administration ensures liposome directly targeting fibroblasts and collagen fibers. Fibroblasts internalize the liposomes, allowing the drug to exert a cytotoxic effect.

Common adverse effects of 5-Fu include gastrointestinal reactions, alopecia, and skin pigmentation. In our study, no significant gastrointestinal and skin reactions, including hyperpigmentation, were observed due to 5-Fu-Lip. In the future, considering the clinical application of 5-Fu-Lip, more dose-dependent skin cytotoxicity needs to be verified.

Conclusion

In this study, we constructed a liposome carrying 5-Fu to capitalize on the liposome's strong affinity for skin, effective drug release control, and passive targeting capability. Our goal was to provide a more effective method for scar treatment. After analyzing the physical and chemical properties as well as the pharmacokinetics, 5-Fu-Lip was proved to be stable and safe. It demonstrated superior ability in inhibiting scar fibroblast proliferation, migration, collagen deposition, and fibroblast-to-myofibroblast conversion, while also reducing microvessel formation compared to free 5-Fu. These findings were further validated in animal experiments. However, the lack of exploration of the 5-Fu-Lip mechanism and the lack of observing the efficacy in actual clinical practice are limitations of this study. In the future, it will be more helpful for commercial production if the biosafety of the drug-carrying material can be ensured and the drug-release ability can be verified in clinical trials.

In conclusion, the satisfactory drug release effect of 5-Fu-Lip can provide continuous efficacy at a low dose and low toxicity, improving scar treatment outcomes while alleviating patients' adverse effects such as itching and pain. Therefore, we anticipate that 5-Fu-Lip may be beneficial in scar treatment.

Acknowledgments

We would like to specially thank Hunan Engineering Research Center of Skin Health and Disease (Changsha, China) for providing HFF-1 and HUVECs cell lines.

Funding

This study was supported by grants from the National Natural Science Foundation of China (No. 82103476) and Mobile Healthcare: Ministry of Education, China Mobile Joint Laboratory (CMCMII-202200349).

Disclosure

The authors report no conflicts of interest in this work.

References

1. Ogawa R. Keloid and hypertrophic scars are the result of chronic inflammation in the reticular dermis. *Int J Mol Sci*. 2017;18(3):606. doi:10.3390/ijms18030606
2. Sinha S, Sparks HD, Labit E, et al. Fibroblast inflammatory priming determines regenerative versus fibrotic skin repair in reindeer. *Cell*. 2022;185(25):4717–4736.e25. doi:10.1016/j.cell.2022.11.004
3. Jeschke MG, Wood FM, Middelkoop E, et al. Scars. *Nat Rev Dis Primers*. 2023;9(1):64. doi:10.1038/s41572-023-00474-x
4. Wolfram D, Tzankov A, Pülzl P, et al. Hypertrophic scars and keloids--a review of their pathophysiology, risk factors, and therapeutic management. *Dermatol Surg*. 2009;35(2):171–181. doi:10.1111/j.1524-4725.2008.34406.x

5. Sen CK, Gordillo GM, Roy S, et al. Human skin wounds: a major and snowballing threat to public health and the economy. *Wound Repair Regen*. 2009;17(6):763–771. doi:10.1111/j.1524-475X.2009.00543.x
6. desJardins-Park HE, Chinta MS, Foster DS, et al. Fibroblast heterogeneity in and its implications for plastic and reconstructive surgery: a basic science review. *Plast Reconstr Surg Glob Open*. 2020;8(6):e2927. doi:10.1097/GOX.0000000000002927
7. Guo T, Mousavi HS, Monga V, Adaptive transform domain image super-resolution via orthogonally regularized deep networks. IEEE Trans Image Process; 2019.
8. Gold MH, McGuire M, Mustoe TA, et al. Updated international clinical recommendations on scar management: part 2--algorithms for scar prevention and treatment. *Dermatol Surg*. 2014;40(8):825–831. doi:10.1111/dsu.0000000000000050
9. Sun P, Lu X, Zhang H, et al. The efficacy of drug injection in the treatment of pathological scar: a network meta-analysis. *Aesthetic plastic Surgery*. 2021;45(2):791–805. doi:10.1007/s00266-019-01570-8
10. Li Y, Zhang D, Hang B, et al. The efficacy of combination therapy involving excision followed by intralesional 5-fluorouracil and betamethasone, and radiotherapy in the treatment of keloids: a randomized controlled trial. *Clin Cosmet Invest Dermatol*. 2022;15:2845–2854. doi:10.2147/CCID.S388717
11. Mokos ZB, Jović A, Grgurević L, et al. Current therapeutic approach to hypertrophic scars. *Front Med*. 2017;4:83. doi:10.3389/fmed.2017.00083
12. Bik L, Sangers T, Greveling K, et al. Efficacy and tolerability of intralesional bleomycin in dermatology: a systematic review. *J Am Acad Dermatol*. 2020;83(3):888–903. doi:10.1016/j.jaad.2020.02.018
13. Shaarawy E, Hegazy RA, Abdel Hay RM. Intralesional botulinum toxin type A equally effective and better tolerated than intralesional steroid in the treatment of keloids: a randomized controlled trial. *J Cosmet Dermatol*. 2015;14(2):161–166. doi:10.1111/jocd.12134
14. Chalabi-Dchar M, Fenouil T, Machon C, et al. A novel view on an old drug, 5-fluorouracil: an unexpected RNA modifier with intriguing impact on cancer cell fate. *NAR Cancer*. 2021;3(3):zcab032. doi:10.1093/narcan/zcab032
15. Searle T, Al-Niaimi F, Ali FR. 5-fluorouracil in dermatology: the diverse uses beyond malignant and premalignant skin disease. *Dermatologic Surg*. 2021;47(3):e66–e70. doi:10.1097/DSS.0000000000002879
16. Kontochristopoulos G, Stefanaki C, Panagiotopoulos A, et al. Intralesional 5-fluorouracil in the treatment of keloids: an open clinical and histopathologic study. *J Am Acad Dermatol*. 2005;52(3 Pt 1):474–479. doi:10.1016/j.jaad.2004.09.018
17. Bijlard E, Steltenpool S, Niessen FB. Intralesional 5-fluorouracil in keloid treatment: a systematic review. *Acta Derm Venereol*. 2015;95(7):778–782. doi:10.2340/00015555-2106
18. Diasio RB, Harris BE. Clinical pharmacology of 5-fluorouracil. *Clin. Pharmacokinet.* 1989;16(4):215–237. doi:10.2165/00003088-198916040-00002
19. Khalid FA, Mehrose MY, Saleem M, et al. Comparison of efficacy and safety of intralesional triamcinolone and combination of triamcinolone with 5-fluorouracil in the treatment of keloids and hypertrophic scars: randomised control trial. *Burns*. 2019;45(1):69–75. doi:10.1016/j.burns.2018.08.011
20. Khan MA, Bashir MM, Khan FA. Intralesional triamcinolone alone and in combination with 5-fluorouracil for the treatment of keloid and hypertrophic scars. *J Pak Med Assoc*. 2014;64(9):1003–1007.
21. Lei L, Bai Y, Qin X, et al. Current understanding of hydrogel for drug release and tissue engineering. *Gels*. 2022;8(5):301. doi:10.3390/gels8050301
22. Ju Y, Liu X, Ye X, et al. Nanozyme-based remodeling of disease microenvironments for disease prevention and treatment: a review. *ACS Appl. Nano Mater.* 2023;6(15):13792–13823. doi:10.1021/acsanm.3c02097
23. Agrahari V, Burnouf PA, Burnouf T, Agrahari V. Nanoformulation properties, characterization, and behavior in complex biological matrices: challenges and opportunities for brain-targeted drug delivery applications and enhanced translational potential. *Adv Drug Deliv Rev*. 2019;148:146–180. doi:10.1016/j.addr.2019.02.008
24. Jain RK, Stylianopoulos T. Delivering nanomedicine to solid tumors. *Nat Rev Clin Oncol*. 2010;7(11):653–664. doi:10.1038/nrclinonc.2010.139
25. Yingchoncharoen P, Kalinowski DS, Richardson DR. Lipid-based drug delivery systems in cancer therapy: what is available and what is yet to come. *Pharmacol Rev*. 2016;68(3):701–787. doi:10.1124/pr.115.012070
26. Wang M, Chen L, Huang W, et al. Improving the anti-keloid outcomes through liposomes loading paclitaxel–cholesterol complexes. *Int J Nanomed*. 2019;14:1385–1400. doi:10.2147/IJN.S195375
27. Shan H, Sun X, Liu X, et al. One-step formation of targeted liposomes in a versatile microfluidic mixing device. *Small*. 2023;19(7):e2205498. doi:10.1002/smll.202205498
28. He Y, Zhang S, Bao W, et al. An improved explants culture method: sustainable isolation of keloid fibroblasts with primary characteristics. *J Cosmet Dermatol*. 2022;21(12):7131–7139. doi:10.1111/jocd.15416
29. Zhang Q, Shi L, He H, et al. Down-regulating scar formation by microneedles directly via a mechanical communication pathway. *ACS Nano*. 2022;16(7):10163–10178. doi:10.1021/acsnano.1c11016
30. Zhang J, Zheng Y, Lee J, et al. A pulsatile release platform based on photo-induced imine-crosslinking hydrogel promotes scarless wound healing. *Nat Commun*. 2021;12(1):1670. doi:10.1038/s41467-021-21964-0
31. Ogawa R, Akita S, Akaishi S, et al. Diagnosis and treatment of keloids and hypertrophic scars-japan scar workshop consensus document 2018. *Burns Trauma*. 2019;7:39. doi:10.1186/s41038-019-0175-y
32. Longley DB, Harkin DP, Johnston PG. 5-fluorouracil: mechanisms of action and clinical strategies. *Nat Rev Cancer*. 2003;3(5):330–338. doi:10.1038/nrc1074
33. Cheng R, Liu L, Xiang Y, et al. Advanced liposome-loaded scaffolds for therapeutic and tissue engineering applications. *Biomaterials*. 2020;232:119706. doi:10.1016/j.biomaterials.2019.119706
34. Qin Z, Chen F, Chen D, et al. Transdermal permeability of triamcinolone acetonide lipid nanoparticles. *Int J Nanomed*. 2019;14:2485–2495. doi:10.2147/IJN.S195769
35. Chen YY, Lu Y-H, Ma C-H, et al. A novel elastic liposome for skin delivery of papain and its application on hypertrophic scar. *Biomed Pharmacother*. 2017;87:82–91. doi:10.1016/j.biopha.2016.12.076
36. Phatale V, Vaiphei KK, Jha S, et al. Overcoming skin barriers through advanced transdermal drug delivery approaches. *J Control Release*. 2022;351:361–380. doi:10.1016/j.jconrel.2022.09.025
37. Sackmann EK, Fulton AL, Beebe DJ. The present and future role of microfluidics in biomedical research. *Nature*. 2014;507(7491):181–189. doi:10.1038/nature13118

38. Shah S, Dhawan V, Holm R, et al. Liposomes: advancements and innovation in the manufacturing process. *Adv Drug Deliv Rev*. 2020;154-155:102–122. doi:10.1016/j.addr.2020.07.002
39. Shah VV, Aldahan AS, Mlacker S, et al. 5-fluorouracil in the treatment of keloids and hypertrophic scars: a comprehensive review of the literature. *Dermatol Ther*. 2016;6(2):169–183. doi:10.1007/s13555-016-0118-5
40. Large DE, Abdelmessih RG, Fink EA, et al. Liposome composition in drug delivery design, synthesis, characterization, and clinical application. *Adv Drug Deliv Rev*. 2021;176:113851. doi:10.1016/j.addr.2021.113851
41. Grabowski G, Pacana MJ, Chen E. Keloid and hypertrophic scar formation, prevention, and management: standard review of abnormal scarring in orthopaedic surgery. *J Am Acad Orthop Surg*. 2020;28(10):e408–e414. doi:10.5435/JAAOS-D-19-00690
42. Hackett TL, Vriesde NRTF, AL-Fouadi M, et al. The role of the dynamic lung extracellular matrix environment on fibroblast morphology and inflammation. *Cells*. 2022;11(2):185. doi:10.3390/cells11020185
43. Gurtner GC, Werner S, Barrandon Y, et al. Wound repair and regeneration. *Nature*. 2008;453(7193):314–321. doi:10.1038/nature07039
44. Korntner S, Lehner C, Gehwolf R, et al. Limiting angiogenesis to modulate scar formation. *Adv Drug Deliv Rev*. 2019;146:170–189. doi:10.1016/j.addr.2018.02.010
45. Wietecha MS, DiPietro LA. Therapeutic Approaches to the Regulation of Wound Angiogenesis. *Adv Wound Care*. 2013;2(3):81–86. doi:10.1089/wound.2011.0348
46. Nunez JH, Strong AL, Comish P, et al. A review of laser therapies for the treatment of scarring and vascular anomalies. *Adv Wound Care*. 2023;12(2):68–84. doi:10.1089/wound.2021.0045
47. Zhou QD, Gong J, Bi J, et al. KGF-2 regulates STAP-2-mediated signal transducer and activator of transcription 3 signaling and reduces skin scar formation. *J Invest Dermatol*. 2022;142(7):2003–+. doi:10.1016/j.jid.2021.12.018
48. Tian S, Zheng Y, Xiao S, et al. Ivermectin inhibits cell proliferation and the expression levels of type I collagen, α-SMA and CCN2 in hypertrophic scar fibroblasts. *Mol Med Rep*. 2021;24(1). doi:10.3892/mmr.2021.12127.
49. Seo CH, Cui HS, Kim JB. Calpastatin-mediated inhibition of calpain ameliorates skin scar formation after burn injury. *Int J Mol Sci*. 2021;22(11):5771. doi:10.3390/ijms22115771
50. Hsieh SC, Wu -C-C, Hsu S-L, et al. Gallic acid attenuates TGF-β1-stimulated collagen gel contraction via suppression of RhoA/Rho-kinase pathway in hypertrophic scar fibroblasts. *Life Sci*. 2016;161:19–26. doi:10.1016/j.lfs.2016.07.011
51. Hwangbo C, Tae N, Lee S, et al. Syntenin regulates TGF-β1-induced smad activation and the epithelial-to-mesenchymal transition by inhibiting caveolin-mediated TGF-β type I receptor internalization. *Oncogene*. 2016;35(3):389–401. doi:10.1038/onc.2015.100
52. Rippa AL, Kalabusheva EP, Vorotelyak EA. Regeneration of dermis: scarring and cells involved. *Cells*. 2019;8(6):607. doi:10.3390/cells8060607
53. Zhang Y, Lin X, Chu Y, et al. Dapagliflozin: a sodium-glucose cotransporter 2 inhibitor, attenuates angiotensin II-induced cardiac fibrotic remodeling by regulating TGFβ1/Smad signaling. *Cardiovasc Diabetol*. 2021;20(1):121. doi:10.1186/s12933-021-01312-8
54. Wu W, Wang X, Yu X, et al. Smad3 signatures in renal inflammation and fibrosis. *Int J Biol Sci*. 2022;18(7):2795–2806. doi:10.7150/ijbs.71595
55. Du Y, Xiao H, Wan J, et al. Atorvastatin attenuates TGF-β1-induced fibrogenesis by inhibiting smad3 and MAPK signaling in human ventricular fibroblasts. *Int J Mol Med*. 2020;46(2):633–640. doi:10.3892/ijmm.2020.4607
56. Zhao J, Han M, Zhou L, et al. TAF and TDF attenuate liver fibrosis through NS5ATP9, TGFβ1/Smad3, and NF-κB/NLRP3 inflammasome signaling pathways. *Hepatol Int*. 2020;14(1):145–160. doi:10.1007/s12072-019-09997-6
57. Mascharak S, desJardins-Park HE, Davitt MF, et al. Preventing engrailed-1 activation in fibroblasts yields wound regeneration without scarring. *Science*. 2021;372(6540):6540. doi:10.1126/science.aba2374
58. Gandek TB, van der Koog L, Nagelkerke A. A Comparison of cellular uptake mechanisms, delivery efficacy, and intracellular fate between liposomes and extracellular vesicles. *Adv Healthc Mater*. 2023;12(25):e2300319. doi:10.1002/adhm.202300319
59. Un K, Sakai-Kato K, Oshima Y, et al. Intracellular trafficking mechanism, from intracellular uptake to extracellular efflux, for phospholipid/cholesterol liposomes. *Biomaterials*. 2012;33(32):8131–8141. doi:10.1016/j.biomaterials.2012.07.030